INTERNATIONAL JOURNAL OF INTEGRATED ENGINEERING
ISSN: 2229-838X e-ISSN: 2600-7916

IJIE

Vol. 16 No. 6 (2024) 294-309
https://publisher.uthm.edu.my/ojs/index.php/ijie

Predictive Model and Optimisation of MQL Mist Flow Velocity Through CFD Analysis

Zulaika Zulkifli[1], Nurul Hayati Abdul Halim[1]*, Zainoor Hailmee Solihin[1], Nur Fatini Mohamad Fauzee[1], Musfirah Abdul Hadi[2]

[1] *School of Mechanical Engineering, College of Engineering, Universiti Teknologi MARA, 40450, Shah Alam, Selangor, MALAYSIA*

[2] *Faculty of Manufacturing and Mechatronic Engineering, Universiti Malaysia Pahang, 26600, Pekan, Pahang, MALAYSIA*

*Corresponding Author: hayatihalim@uitm.edu.my
DOI: https://doi.org/10.30880/ijie.2024.16.06.028

Article Info

Received: 11 May 2024
Accepted: 24 November 2024
Available online: 29 December 2024

Keywords

Minimum Quantity Lubricant (MQL), Computational Fluid Dynamics (CFD), Box-Behnken, Response Surface Methodology (RSM), High-Speed Milling, MQL Mist Flow

Abstract

Minimum Quantity Lubricant (MQL) is a sustainable machining method offering better lubrication and cooling efficiency for high machining performances. To further enhance its sustainability, this study is conducted based on the Computational Fluid Dynamic (CFD) analysis on an MQL delivery model using Treated Recycled Cooking Oil (TRCO) to simulate a high-speed cutting process. The main aim is to optimise the mist flow velocity which leads to optimum penetration of lubrication deep into the cutting zone. Through the design of experiment approach under the Box-Behnken Response Surface Methodology (RSM) method, 13 sets of parameters were simulated with controlled factors of oil flow rate (50-150 ml/hr), nozzle distance (20-60 mm), and nozzle diameter (1-2 mm). Then, Analysis of Variance (ANOVA) was applied to investigate how the controlled factors influence the response. The simulation works resulted in the MQL mist flow reaching velocity that varied from 15.43 to 115.52 m/s. The ANOVA revealed that the response is significantly influenced by nozzle distance, nozzle diameter, and the interaction between them. The highest velocity was generated at minimum nozzle distance and maximum nozzle diameter. Contrary, maximum nozzle distance and minimum nozzle diameter generated the lowest value. The flowback or rebound conditions of the mist flow at different flow velocities were also visualized and discussed with the aid of CFD contour images. Through optimization, the optimum MQL mist flow velocity at 115.34 m/s is predicted at; oil flow rate: 100 ml/hr, nozzle diameter: 2 mm, and nozzle distance: 20 mm from the tool edge. This optimum MQL mist flow is vital for high-speed cutting due to massive generation of friction and heat that require deep penetration of the lubricant into the cutting edge for maximum heat dissipation.

1. Introduction

In metal cutting, one of the major concerns is high cutting temperature and cutting force due to friction and heat that are inherently generated particularly during high-speed machining of hard materials. The main cause is due to poor dissipation of heat from the cutting zone which then accumulates at the cutting tool edge and workpiece [1]. This situation leads to excessive tool wear, poor surface finish, and work hardening which are heat-dependent and also interdependent [2]–[4]. This phenomenon happens in any conventional machining but worsens in dry cutting with the absence of lubrication and cooling effect. To overcome the issue, a conventional flood cooling method is widely applied. However, the usage of a great amount of lubricant in flood cutting and improper handling and disposal methods have negative impacts on the environment and human health which make it impractical to be utilised [5]. Thus, a sustainable Minimum Quantity Lubrication (MQL) has been introduced with a cost-effective and environmentally friendly alternative to dry and flood machining. MQL is regarded as a sustainable approach as it utilises only 6 to 100 mL/h of lubricant at the cutting zone, as compared to 1000 L/min in flood cutting [6]. The MQL system uses a mixture of pressurised air and cutting fluid which supplies it directly into the cutting zone by atomising and spraying technique. The extreme reduction in lubricant quantities results in nearly dry workpieces and chips. Yet, it efficiently provides a cooling and lubrication effect to disseminate heat and immediately improve machining performances [7]-[8].

Literature shows that the MQL cutting performance highly depends on the effectiveness of the mist to penetrate deep into the cutting zone [9]-[10]. Good penetration means the mist has successfully reached and is evenly distributed across the entire contact area of tool-workpiece and tool-chip interfaces, particularly along the tool edge. At the same time, it provides consistent and sufficient cooling and lubrication effect which creates a machining environment with effective friction, heat, and chip removal, preventing localised overheating or wear. It was reported that the mist flow velocity is one of the important mist flow behaviours as it significantly influences the penetration level. According to Rahim et al. [11], high mist flow velocity facilitates deep penetration of the lubricant to reduce friction between interfaces. This is because it allows the lubricant to continuously flow faster and hit the cutting zone effectively. Paralely, Rahim, and Dorairaju [12] reported that the mist particles with low velocity have led to less cooling effect due to the tendency of condensation along its travel. When referring to Zhu et al. [13], they highlighted the negative impact of high mist flow velocity as it also has the potential to reduce the penetration through rebounding effect, where the flow back of the mist happens as it hits the cutting surface. Thus, there must be an optimum value or a balance between low and high mist flow velocity for the MQL machining. Literatures have also suggested that MQL system parameters such as oil flow rate [14], [15], air pressure [16], spray angle, and nozzle distance [14]-[15] are responsible for affecting the velocity of the mist spray.

Another critical factor that controls the MQL mist behaviour is the nozzle used in the MQL supply system. The nozzle plays an important role in supplying the mist of fluid directly into the cutting zone. Thus, its variables in terms of geometry, position, and distance are continuously gaining interest in study. For instance, Liu et al. [17] found that oil flow rate and spraying distance are among the critical factors to be controlled as they affect the performances of end milling processes. Referring to Wang et al. [18] and Pereira et al. [19], they mentioned that appropriate nozzle designs and positions are essential to ensure the cutting fluids or coolant penetrates deep into the tool-chip interface. Effectively, it hinders the increase of cutting temperatures as well as rapid tool wear rates. In addition, Pereira et al. [19] suggested that the right diameter of the nozzle is essential to be analysed and identified so that the mist can reach the tooltip during cutting without being spread into the atmosphere. Meanwhile, Zaman and Dhar [20] stated that turning with double jet nozzles of the MQL system resulted in better surface roughness, and tool life as well as a reduction of cutting temperatures as compared to single jet nozzle. Thus, it can be said that the variations of the nozzle such as its geometry, design, and position play an important role in the machining performance; hence, it must be chosen correctly to ensure efficient lubrication supply.

Previous studies on MQL machining revealed that the parametric studies of fluid flow analysis of the MQL mist flow behaviour are still lacking, particularly for multiphase flow that is physically complex and not easily captured and analysed experimentally. Indeed, how the MQL system parameters influence the mist performances is still questionable and continuously gaining interest from researchers. Past research focused more on analysing MQL machining performances experimentally such as on the aspects of tool wear rate, surface roughness, and cutting force as they are measurable by specific measuring devices. Thus, this present work aims to fill this gap by utilising Computational Fluid Dynamics (CFD) modeling of ANSYS Fluent to analyse and optimise the MQL mist flow velocity in high-speed milling. CFD provides a detailed visualisation of the flow characteristics, mist formation, dispersion, and interaction with surfaces, which is challenging to observe visually [16], [21]-[22]. In a study by Pereira et al. [19], they applied CFD to analyse the performance of a new nozzle adaptor with different outlet diameters of cryoMQL application where the study focused on validating the flow velocity. Meanwhile, Najiha et al. [16] applied CFD to investigate the temperature profile and oil droplet behaviour in the cutting zone of the turning process with variations of MQL parameters. In this study, the design of the experiment approach under the response surface methodology of the Box Behnken method was utilised to design the controlled variables. For a thorough analysis of the interdependencies of the controlled variables, the statistical method of Analysis of Variance (ANOVA) was applied. To further enhance the sustainability of MQL machining, Treated Recycled Cooking Oil (TRCO) is used to replace commercial cutting oil.

Int. Journal of Integrated Engineering Vol. 16 No. 6 (2024) p. 294-309

2. Methodology

In this study, the influence factors of the MQL system which are oil flow rate, nozzle diameter, and nozzle distance on the MQL mist flow velocity were thoroughly analysed through simulation works using CFD ANSYS Fluent software. The concept of a 2D-symmetrical MQL delivery model used in this study is shown in Figure 1 where it was established by referring to Najiha et al. [24], Pereira et al. [19], and Subramani et al. [25]. The preliminary study on mesh independence was conducted earlier in order to identify the optimum mesh setting for this study [26].

2.1 Mathematical Model

The mathematical model established in this study was based on the MQL delivery system design concept as shown in Figure 1a. A detailed configuration of the MQL system as shown in Figure 1b portrays the channel of each fluid which are air pressure as input 1 at inlet 1 and oil lubricant as input 2 at inlet 2. A multiphase flow was implicated as two different fluid properties were channeled into the MQL nozzle before the mixture in the form of mist was dispersed directly into the contact zone of the tool-workpiece interface. The mathematical model was derived from the Navier Stokes equation which is known for the 3-dimension flow system and consists of the Continuity equation as in Equation 1 and the Momentum equation as in Equation 2. These equations are commonly used for fluid flow to study and analyse the flow behaviour and condition.

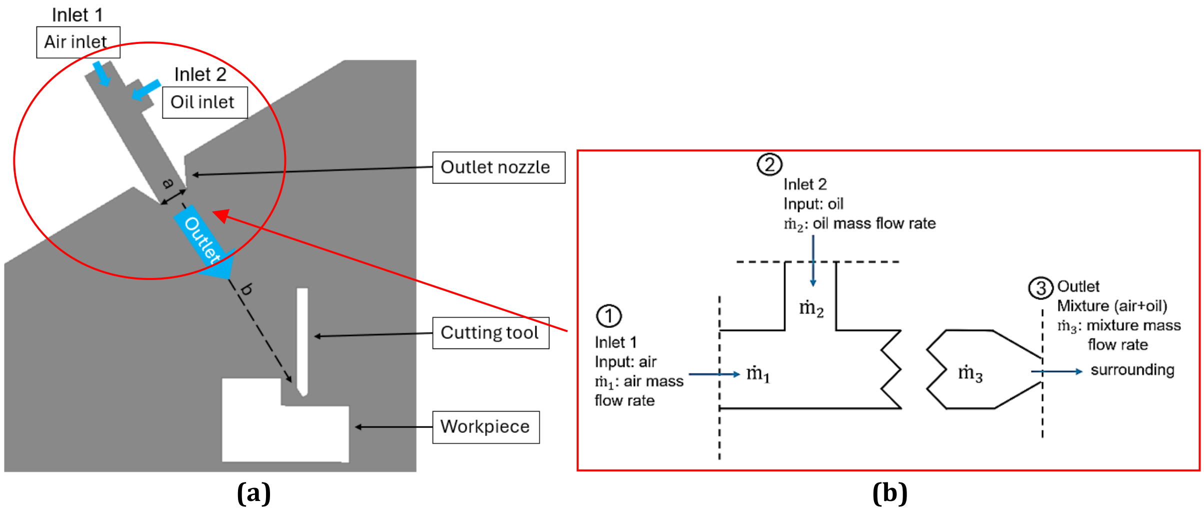

Fig. 1 *The schematic diagram of (a) MQL model and boundary conditions in CFD; and (b) MQL mist flow system*

The Navier-Stokes equation was derived into Bernoulli's equation as it is suitable for a linear streamline flow. There are five (5) assumptions considered for the MQL flow conditions which are (i) unidirectional, (ii) steady, (iii) incompressible, (iv) frictionless, and (v) adiabatic.

For the Continuity equation:

$$\frac{\partial \rho}{\partial t} + \overrightarrow{\nabla \rho} \cdot \vec{v} = 0 \tag{1}$$

For the Momentum equation:

$$\rho \frac{\partial \vec{v}}{\partial t} + \rho(\vec{v} \cdot \vec{\nabla})\vec{v} = \overline{\rho \vec{g}} - \vec{\nabla} p + \mu \vec{\nabla}^2 \vec{v} \tag{2}$$

Where v, μ, p, and $\vec{g}$ are denoted as velocity, viscosity, pressure, and gravity. The MQL flow is assumed incompressible where the density (ρ) is constant with respect to time and space. Thus, the term $\frac{\partial \rho}{\partial t}$ is neglected from Equation 1 and derived into Equation 3.

$$\vec{\nabla}\vec{v} = 0 \tag{3}$$

In Bernoulli's equation principle, the flow is displaced between distance, s in a linear path and the trajectory of the flow is expressed as a segment. The $d\vec{s}$ represents the length of the flow from the inlet to the outlet in one direction. As shown in Figure 1b, there are two inlet points which are point 1 for air inlet and point 2 for oil lubricant inlet. Both flows are channeled into point 3 which is the outlet for the MQL mist flow. Thus, to meet the second condition of Bernoulli's, a segment $d\vec{s}$ is projected into Equation 2. The equation in vectors is converted into scalar where now a series of variables are as shown in Equation 4.

$$\rho \frac{\partial v}{\partial t}.ds + \rho(v.\nabla)v.ds = \rho g.ds - \nabla p.ds + \mu\nabla^2 v.ds \tag{4}$$

The MQL flow is assumed steady whereas there are no changes in time. Meanwhile, it is also assumed the flow is frictionless as the flow viscosity is negligible, thus $\mu\nabla^2 v.ds$ = 0. To simplify the equation, both sides are divided by *ds* and developed into Equation 5.

$$\rho v dv = -\rho g\, dz - dP \tag{5}$$

With the assumption that the flow is adiabatic with ρ = constant, the flow is considered as no interaction with the heat transfer. The derivation is involved with the integration work that involves the differential equation with a proper boundary condition to acquire the actual behaviour such as velocity, pressure, and density throughout the fluid domain. This information is essential for predicting flow aspects like flow patterns. The trajectory distance is assumed from the initial as *a* and the end as *b*, and the boundary condition is taken from the path of *a* to *b*. Then, integrate them within this distance for Equation 6 which is expressed as $\rho \int_a^b V dV = -\rho \int_a^b g dz - \int_a^b dP$. The flow is assumed it be not affected by gravity as the fluid flows horizontally, thus $-\int_a^b \rho g dz = 0$=0. A completed Bernoulli's equation for the MQL system delivery flow is derived in Equation 6.

For the Bernoulli's equation:

$$\Delta P + \frac{\rho \Delta v^2}{2} = 0 \tag{6}$$

Bernoulli's equation is now applied to the fluid flow in the MQL delivery system. By referring to the schematic diagram in Figure 1 and assuming there is no leaking in the system; $\sum \dot{m}_{in} = \sum \dot{m}_{out}$. Therefore, the fluid flow in the system is expressed in Equation 7.

$$\dot{m}_3 = \dot{m}_1 + \dot{m}_2 \tag{7}$$

Where $\dot{m}_1$, $\dot{m}_2$ and $\dot{m}_3$ are the mass flow rates of inlet 1, inlet 2, and outlet, respectively. Subsequently, Equation 7 is derived into $\rho_3 v_3 A_3 = \rho_1 v_1 A_1 + \rho_2 v_2 A_2$, where *ρ*, *v*, and *A* are denoted as density, velocity, and nozzle area, respectively. From this equation, there are two unknown parameters which are output density (ρ_3) and output velocity (v_3) that this study needs to solve. By rearranging the equations, Equation 8 is derived for the unknown output density (ρ_3).

$$\rho_3 = \frac{\rho_1 v_1 A_1 + \rho_2 v_2 A_2}{v_3 A_3} \tag{8}$$

Bernoulli's equation in Equation 6 is rearranged according to the MQL delivery system where the inlet is equal to the outlet resulting in Equation 9. The term $\Delta P_1 + \frac{\rho_1 \Delta v_1^2}{2}$ represents the flow at inlet 1 which is the air pressure, while $\Delta P_2 + \frac{\rho_2 \Delta v_2^2}{2}$ indicates the flow at inlet 2 which is the oil lubricant, and $\frac{\rho_3 \Delta v_3^2}{2}$ stands for the output parameters which is the MQL mist flow. The Bernoulli's equation in the MQL delivery system is:

$$\Delta P_1 + \frac{\rho_1 \Delta v_1^2}{2} + \Delta P_2 + \frac{\rho_2 \Delta v_2^2}{2} = \Delta P_3 + \frac{\rho_3 \Delta v_3^2}{2} = 0 \tag{9}$$

where P_1, P_2, and P_3 are pressure for air, oil lubricant, and MQL mist flow, respectively. Now, the derivation from Equation 8 is introduced into Equation 9 which generates Equation 10. Further manipulation then results in Equation 11 which represents v_3 as the unknown output velocity that requires to be solved.

$$\left[2\Delta P_3 + \left(\frac{\rho_1 v_1 A_1 + \rho_2 v_2 A_2}{v_3 A_3}\right)\Delta {v_3}^2\right] = \left(\Delta P_1 + \frac{\rho_1 \Delta {v_1}^2}{2}\right) + \left(\Delta P_2 + \frac{\rho_2 \Delta {v_2}^2}{2}\right) \tag{10}$$

$$v_3 = \frac{(2\Delta P_1 A_3 + \rho_1 \Delta {v_1}^2 A_3) + (2\Delta P_2 A_3 + \rho_2 \Delta {v_2}^2 A_3) - (2\Delta P_3 A_3)}{(\rho_1 v_1 A_1 + \rho_2 v_2 A_2)} \tag{11}$$

Where the parameters of the output velocity (v_3) are influenced by various input factors of v_1, v_2, P_1, P_2, ρ_1, and ρ_2. From the equation, the variables of P_1, P_2, P_3, and areas of A_1, A_2, and A_3, are treated as constant parameters as shown in Table 1.

Table 1 *MQL constant parameters*

Variables	Values
Air pressure, P_1 (bar)	4
Oil lubricant pressure, P_2 (bar)	0
MQL mist flow pressure, P_3 (bar)	1
Air nozzle area, A_1 (m^2)	3.14×10^{-6}
Oil nozzle area, A_2 (m^2)	3.14×10^{-6}
MQL mist flow nozzle area, A_3 (m^2)	3.14×10^{-6}

2.2 Governing Equation and CFD Modeling

The governing equation used in CFD is based on the Navier-Stokes equation, with a set of partial differential equations involved which are continuity and momentum equations. The Finite Volume Method (FVM) in Ansys Fluent is used numerically to solve the governing equations in CFD. The FVM applies the conservation rules of mass, momentum, and energy at each control volume after discretising the computational domain into tiny control volumes. Only the laws of mass and momentum are applied in this research. Once convergence is attained, the resultant system of equations is solved again. Meanwhile, modelling in CFD involves several steps, including setting up the model geometry, defining the boundary conditions, specifying the fluid properties, and selecting an appropriate turbulence model. The boundary conditions are where the inlet of air and oil lubricant, as well as the outlet of MQL mist flow, are defined in the CFD.

In CFD work, Volume of Fluid (VOF) is used to simulate the behaviour of fluids with a multiphase model. VOF is a technique where the two-phase flows are applied separately to track the interface between them at the defined domain. The domain represents the surrounding atmosphere where the mist flow is dispersed in the MQL model. In this study, the VOF was selected since it models the interface between the fluids as a sharp, distinct boundary, and solves the Navier-Stokes equations for both compressed air and lubricant separately in two-phase flow. Mousavi et al. [27] also suggested applying the VOF model as it is suitable for free-surface flow simulation as of the MQL model. In addition, the VOF model is also able to track the volume fraction occupied by fluid and air or other fluids within each computational cell. Thus, the phase volume fraction as in Equation 12 is introduced in order to capture the interface between two phases of air and oil lubricant. Table 2 lists all the controlled parameters for the MQL model, while the value of viscosity and density of the lubricant are referred to Ahmad et al. [28].

In the VOF model, the volume fraction is a sum of all phases presented, with a total value of one. Typically, air is considered as the primary phase with lower density, while oil lubricant is defined as the secondary phase with higher density [29].

$$\alpha_{air} + \alpha_{oil} = 1 \tag{12}$$

Where α_{air} and α_{oil} represent the volume fractions of the air phase and oil lubricant phase, respectively. In this study, the standard k-epsilon turbulence model was chosen based on the Reynolds number calculation, and it is appropriate for studying the centre flow of the MQL mist throughout the domain. The turbulence model which is known for its stability and accuracy in fluid flow and heat transfer simulations consists of two equations which are turbulent kinetic energy (k) and turbulent energy dissipation as shown in Equation 13 and Equation 14, respectively [30].

Table 2 *Parameters for CFD model*

Parameters	Values/Conditions
Geometry	2-dimensional
Models	Multiphase: Volume of Fluid (VOF) Turbulence: Standard k-epsilon
Solver	Pressure-based, steady state
Solution method	SIMPLE pressure coupling scheme
Initialisation	Hybrid
Nozzle air inlet diameter (mm)	2
Nozzle oil inlet diameter (mm)	2
Air density, ρ_1 (kg/m3)	1.225
Air viscosity (kg/m-s)	1.7894×10^{-5}
Air flowrate (l/hr)	72.6
Oil density, ρ_2 (kg/m3)	929.4
Oil viscosity (kg/m-s)	0.297
Air inlet velocity, V_1 (m/s)	231
Air inlet pressure, P_1 (kPa)	400
Oil inlet pressure, P_2 (kPa)	0
Outlet pressure, P_3 (kPa)	0

$$\nabla \cdot \left(\rho \vec{V}\, k\right) = \nabla \cdot \left[\left(\mu + \frac{\mu_t}{\sigma_k}\right) \nabla k\right] + P_k - \rho\varepsilon \tag{13}$$

$$\nabla \cdot \left(\rho \vec{V}\, \varepsilon\right) = \nabla \cdot \left[\left(\mu + \frac{\mu_t}{\sigma_\varepsilon}\right) \nabla \varepsilon\right] + \frac{\varepsilon}{k} C_{1\varepsilon} P_k - \frac{\varepsilon^2}{k} C_{2\varepsilon}\rho \tag{14}$$

Where the laminar viscosity is presented in μ. Equation 15 presents the turbulent viscosity model, μt, while Table 3 shows the constant parameters of the k-ε turbulent model.

$$\mu_t = C_\mu \rho \frac{k^2}{\varepsilon} \tag{15}$$

The Semi-Implicit Method for the Pressure-Linked Equation algorithm type is implemented to solve the scalar variables and simulate the spray behaviour of this solution method.

Table 3 *Constant parameters of k-ε turbulent model*

Parameters	Value
$C_{1\varepsilon}$	1.44
$C_{2\varepsilon}$	1.92
C_μ	0.09

2.3 Design of Experiment (DoE) and Optimization

Table 4 presents the controlled ranges of each factor where they are controlled at 3 levels, and the response is MQL mist flow velocity. To design the parameters for simulation work, the Design of Experiment (DoE) approach through Response Surface Methodology (RSM) under the Box-Behnken method is applied. DoE is a systematic technique for planning and analysing experiments in order to determine the correlation between independent variables and dependent variables [31]. In this study, 13 sets of parameters were generated which were then simulated using CFD Ansys Fluent to identify the measured response. The main aims are to simulate the flow of MQL mist, computably visualise how the mist flow penetrates deep into the cutting zone and identify the variations of MQL mist flow velocity. In the CFD environment, the MQL mist flow that happens in the domain is where the data and results are taken and then analysed.

Table 4 *Controlled parameters and response for MQL mist flow system*

Controlled factors	Controlled levels			Response	Objective
	1	2	3		
Oil flow rate (ml/hr)	50	100	150	MQL mist flow velocity	Maximum
Nozzle diameter (mm)	1	1.5	2		
Nozzle distance (mm)	20	40	60		

After that, a thorough analysis of how the controlled factors influence the responses and the possible interaction between them is performed through statistical analysis of Analysis of Variance (ANOVA). Then, response optimisation is carried out with the aim to maximise the MQL mist flow velocity.

3. Results and Discussion

3.1 Simulation Results

Through CFD analysis of 13 sets of MQL parameters, it was found that the MQL mist flow reaching velocity varies from 15.43 m/s to 115.52 m/s, as listed in Table 5. The highest and lowest velocities are generated in Simulation 2 and Simulation 4, respectively. The average velocity is 55.63 m/s.

Table 5 *Simulation results from CFD analysis*

Simulation No.	Controlled Factors			Measured Response
	A: Oil Flow Rate, Q (ml/hr)	B: Nozzle Diameter, D (mm)	C: Nozzle Distance, d (mm)	Mist flow Velocity, V (m/s)
1	100	1	20	81.37
2	**100**	**2**	**20**	**115.52**
3	50	2	40	58.18
4	**100**	**1**	**60**	**15.43**
5	50	1.5	20	97.11
6	50	1.5	60	22.36
7	150	1.5	20	105.52
8	150	1	40	42.19
9	150	1.5	60	22.86
10	50	1	40	30.32
11	100	2	60	30.16
12	100	1.5	40	43.28
13	150	2	40	58.83

By referring to Figure 3, generally, it can be said that the MQL mist flow velocity increases with the reduction of nozzle distance as in simulations 1, 2, 5, and 7. However, when the distance is increased, it significantly reduces the velocity as in simulations 4, 6, 9, 10, and 11. Meanwhile, the influence of oil flow rate and nozzle diameter is not clear and vague which needs detailed analysis. Kiat et al. [10] believed that a shorter distance between the nozzle and tool-workpiece is more efficient for penetrating the lubricant deep into the contact interfaces as the flow reaches the contact surfaces faster before it starts to lose its kinetic energy. When referring to Van and Nguyen [32], larger nozzle diameters are suggested as they increase mist flow production and allow a large amount of lubricant to disperse from the nozzle and travel longer. However, identifying an optimum nozzle distance and diameter is suggested as the overflow or oversupply also tends to cause a rebound or splashing effect that becomes a disturbance for the flow to enter the cutting zone [33].

3.2 Statistical Analysis by ANOVA for MQL Mist Flow Velocity

Table 6 shows the ANOVA for MQL mist flow velocity. Based on the findings, the model has an F-value of 334.72 with a Prob>F value less than 0.05 which implies that the model is significant. After model reduction, the MQL mist flow velocity is dominantly influenced by factor C as it has the highest F-value at 1726.97, followed by B, C^2, and the interaction between factors *B* and *C*, factor *A*, and interaction between factors *A* and *B*. As suggested by the ANOVA, the interaction between factors *A* and *B* is also included in the model as its p-value is less than 0.1.

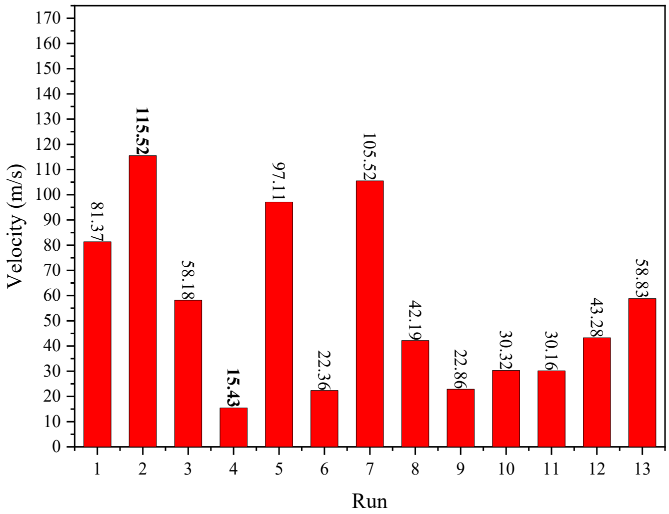

Fig. 3 *MQL mist flow velocity from 13 sets of MQL system parameters*

Table 6 *ANOVA for MQL mist flow velocity (V)*

Source	Sum of squares	df	Mean square	F-value	p-value	
Model	13853.60	6	2308.93	334.72	< 0.0001	significant
A: Oil flow rate (*Q*)	57.41	1	57.41	8.32	0.0279	
B: Nozzle diameter (*D*)	1089.98	1	1089.98	158.01	< 0.0001	
C: Nozzle distance (*d*)	11912.73	1	11912.73	1726.97	< 0.0001	
AB	31.47	1	31.47	4.56	0.0766	
BC	94.28	1	94.28	13.67	0.0101	
C^2	667.72	1	667.72	96.80	< 0.0001	
Residual	41.39	6	6.90			
R^2	0.9970					
Adj. R-Squared	0.9940					
Pred. R- Squared	0.9885					
Adeq. Precision	52.1583					

The ANOVA also found that the R^2 value of the regression model of MQL mist flow velocity is 0.9970 which is very close to the Adjusted R^2 values of 0.9940. Both responses of R^2 and adjusted R^2 values show that the model satisfactorily represents the real relationship between the control factors. The predicted R^2 value is 0.9885, which is in reasonable agreement with the adjusted R^2 as the difference is less than 0.2. The smaller difference indicates a better balance between model complexity and better fit, while the larger difference means the model might overfit the data. Meanwhile, the adequate precision at 52.1583 which is greater than 4 shows that the signal ratio is considered desirable.

A predictive empirical model developed in ANOVA for MQL mist flow velocity is shown in Equation 16. This quadratic model can be used to predict and analyse the effect of controlled factors on the response under the controlled ranges of this study.

$$V = 96.33 + 0.22Q + 53.96D - 4.15d - 0.112QD - 0.486Dd + 0.0368d^2 \tag{16}$$

3.3 Model Diagnostic for MQL Mist Flow Velocity

Model diagnostic is conducted to check the validity and reliability of the quadratic model. It also assists in confirming that the model meets all ANOVA's assumptions and that the data fit and follow certain rules. At the same time, this analysis is also important as it helps to identify any potential issues or outliers that may prevent the model from fitting the data well. To aid the analysis, diagnostic plots which include normal plots of residuals, residuals vs. predicted, and predicted vs. actual are used.

The main function of residual plots is to analyse the residual values for normality and variability [20]. The difference between the actual and predicted response levels is known as the residual. The diagnostic plots for the mist flow velocity as shown in Figure 4 revealed that the residuals are well distributed and fit into the data. In Figure 4a, the normal plot of residuals shows that most of the data are distributed close to the straight line, which indicates the residuals follow a normal distribution in ANOVA. Some points slightly scatter far but there is no significant pattern observed. According to Shaikh et al. [34], the robustness of the analysis of variance is intended to support the normality assumption.

Figure 4b shows the plots of residual vs. predicted, which is used to identify if the variance of residuals is consistent across all levels of predicted values. As shown, the residual plots are randomly scattered around the horizontal line and within the limit of upper and lower red lines. This means that the model is fit with no obvious pattern and has an unusual structure. The reliability of the model is further analysed by comparing the actual value from 13 sets of parameters with the expected values from the linear regression model as plotted in Figure 4c. From the results, all the points fall along a straight line. The errors between predicted and actual results range between 0.09% to 11.02%, with an average of 3.79%. Since the average error is less than 10%, the error is considered low and the model is acceptable, which is fit to do the prediction for the MQL mist flow velocity [35].

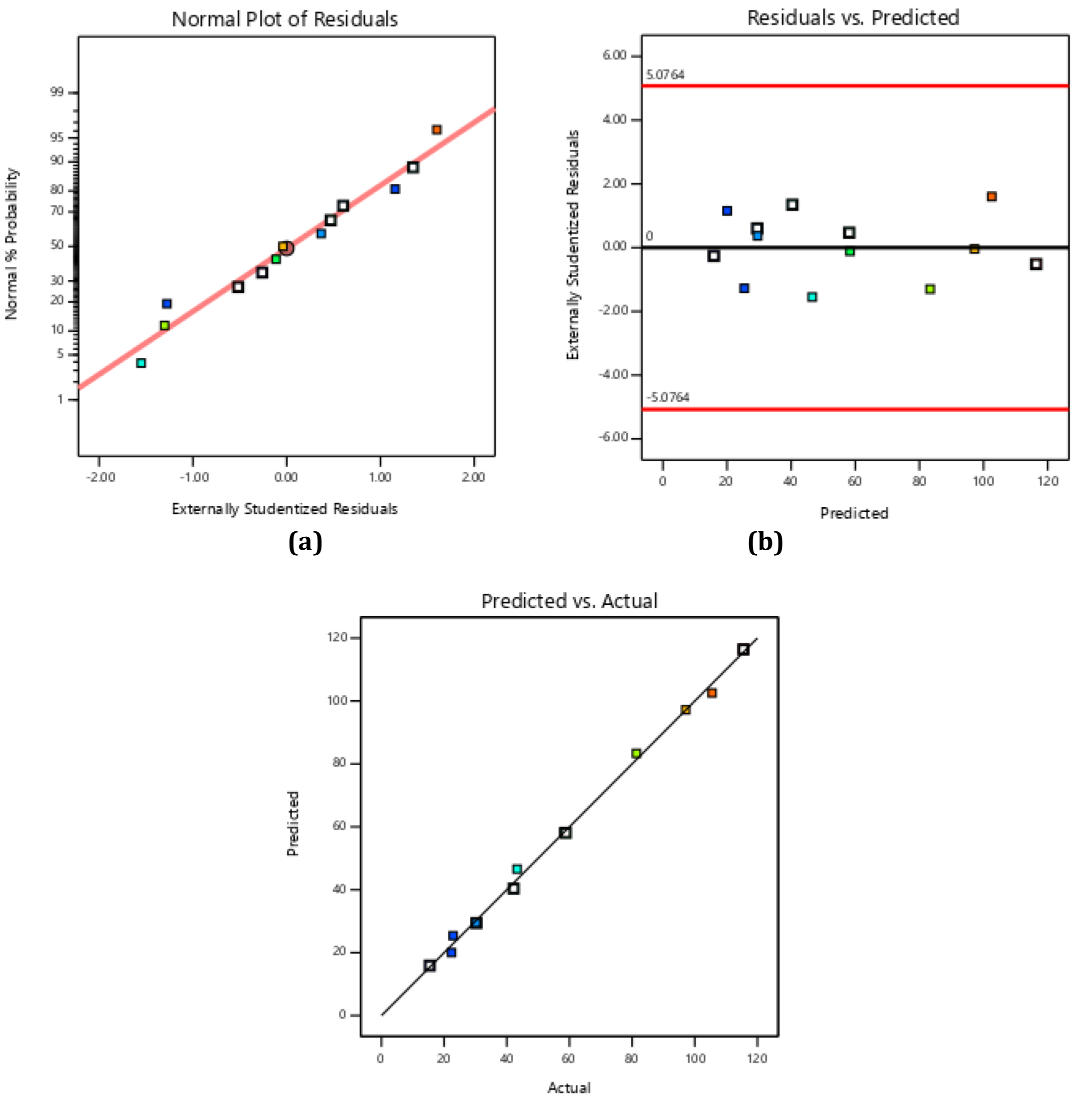

(a) (b)

(c)

Fig. 4 *Model analysis for MQL mist flow velocity model; (a) Normal plots of residuals; (b) Residuals vs. predicted; and (c) Predicted vs. actual*

3.4 Interaction Between Factors for MQL Mist Flow Velocity

The interaction effect between controlled factors on MQL mist flow velocity is more interpretable in the form of a 3D surface model graph. Figure 5 illustrates the significant interactions and how they influence the response.

Figure 5a shows the interaction between factor A (oil flow rate, Q), and B (nozzle diameter, D) on the MQL mist flow velocity. It shows that the increase of both factors values results in a slight increase of the response. The highest flow velocity at V: 58.38 m/s can be achieved at the maximum oil flow rate (Q: 150 ml/hr) and nozzle diameter (D: 2 mm). Meanwhile, the lowest mist flow velocity happened with the reduction of both factors to the minimum points. The shape of the curve also indicates the influence level of both factors on the response. The 3D graph shows a slight inclination with the changes of both factors, indicating that the interaction has less influence as compared to other interactions.

In this study, factor B is seen to provide a more substantial impact as the changes in its value at any point of factor A influence the response. This is aligned with the finding reported by Subramani et al. [25] in enhancing the mean particle velocity of MQL mist flow. According to them, the size of the nozzle diameter controls the amount of lubricant dispersed from the nozzle. However, the oil flow rate also provides a direct influence as it controls the volume of oil being atomised as well as the volume of lubricant delivered per unit of time [33], [36]. Both factors are important to ensure the mist flow provides sufficient coverage of the cutting area, facilitating friction reduction at the contact surfaces. In addition, Chen et al. [36] suggested controlling the airflow rate as the compressed air will break up the oil into micron-sized droplets for better penetration.

The interaction between factor B (nozzle diameter, D) and C (nozzle distance, d) on the mist flow velocity is illustrated in Figure 5b. It was found that both factors interact in opposite ways to influence the response. The highest mist flow velocity is generated at the minimum distance of nozzle (d: 20 mm) from the cutting tool but at the maximum nozzle diameter (D: 2 mm). The same pattern can be seen for the lowest velocity where it is generated at maximum nozzle distance (d: 60 mm), but at minimum nozzle diameter (D: 1 mm). The increase of factor C significantly reduces the velocity, while the changes of factor B are seen to be less influenced. At any factor B value, factor C reduction increases the velocity. The steepest skewness of factor C showed its higher influence on the velocity performance.

This finding is basically aligned with Liu et al. [17] who mentioned the spraying distance as one of the critical controlled parameters to enhance the penetration effect of the MQL mist which relies on its travel velocity. According to them, the distance is also responsible for influencing the diameter of the oil droplet and must be adjusted to match the different cutting parameters and MQL system to be applied. This is important as sufficient lubricant also helps to improve other heat-dependent cutting performances such as surface roughness and cutting force as reported by [28], [33].

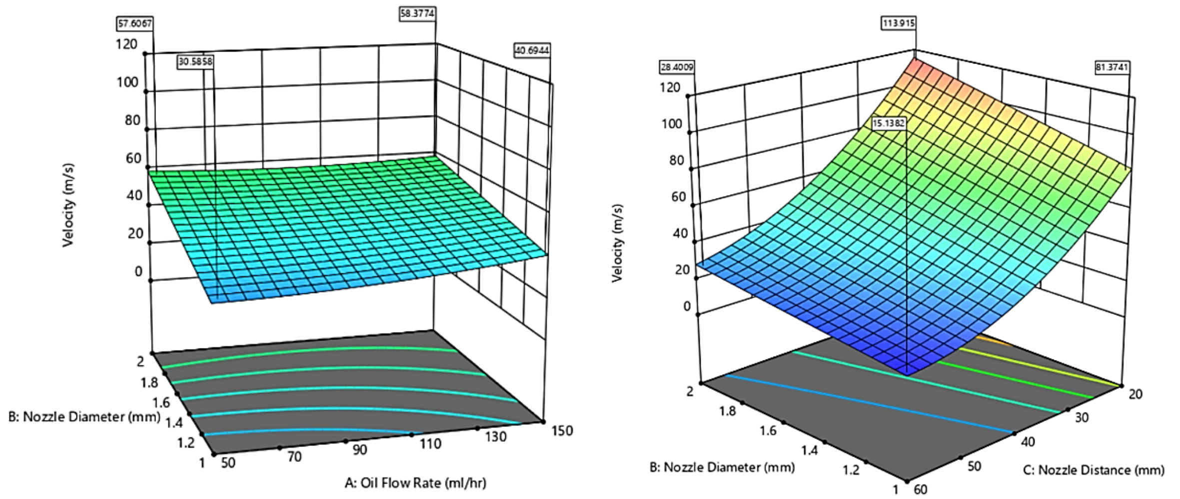

(a) (b)

Fig. 5 *3D graph for; (a) Interaction between A and B; and (b) Interaction between B and C on MQL mist flow velocity*

The increase of MQL mist flow velocity generally provides positive and negative impacts on cutting performances. Supplying the lubricant at high velocity is literally required as it ensures sufficient lubricant is continuously penetrated directly to the cutting point during the cutting. However, it may also cause the mist's rebounding effect, potentially reducing the amount of mist penetrating the cutting region [13]. When referring to Warjito et al. [37], they found that larger nozzle diameters aid in massive fluid flow, which is effective in fluid penetration. However, it also increases consumption and leaves an unpleasant smell and excessive oily marks on the machined surface and machine parts [9].

In MQL, the rebounding or flowback effect refers to a phenomenon where the mist flow bounces back after hitting the cutting point during the cutting process [17]. This occurs as the mist fails to flow deep into the narrow space between the tool-workpiece and tool-chip interface, and it is forced to return to its source. However, the condition and concentration of the rebound effect depend on parameters setups such as oil flow rate, nozzle distance, and nozzle diameter [38]. Therefore, the analysis was further conducted to analyse the two variations of rebound conditions under the maximum and mid-range of velocity values and different nozzle distances. Nozzle distance is varied as it significantly influences the mist flow velocity, as shown in Table 7. In this analysis, the CFD contour images as in Figure 6, and Figure 7 are used to observe the rebound effects and conditions. The red contour indicates the highest velocity value, while the yellow to dark blue contour indicates a decrease in velocity value. The legend in the figures shows the range of contour colours with the velocity values.

Figure 6a shows a CFD contour of Simulation 2 where the highest flow velocity has a sharply pointed flow toward the cutting zone. At the shortest nozzle distance, the highest velocity is generated as it clearly penetrates the narrow area of the cutting zone, which then collides with the obstruction. The collision causes a high intensity of rebound effect that produces a high velocity rebound flow, as shown in Figure 6b. At the same time, this condition also creates a high-pressure zone that builds up at the narrow cutting zone area where the collision happens as shown in Figure 6c. When referring to Chen et al. [36] in their CFD analysis, they observed the same pattern of pressure distribution in the MQL flow field. They found that the high-pressure zone can drastically reduce the mist flow velocity in the cutting zone. However, it can enhance the mist dispersion where more surface area can be covered with the lubricant, particularly along the tool edge, hence reducing friction.

According to Rahim et al. [11] and Yang et al. [39], effective penetration from high mist flow velocity offers sufficient cooling and lubrication effect as well as better chip removal which outperforms the negative impact of the rebound flow. However, further reduction in nozzle distance may reduce the flow velocity so as to the rebound effect, which leads to poor mist flow penetration [40]. In terms of cutting performance, Zhu et al. [13] reported that the closest nozzle distance resulted in higher cutting force and surface roughness due to poor penetration as the droplets rebound from the tool surface. Thus, an optimum nozzle distance is important to be identified for better MQL machining performance.

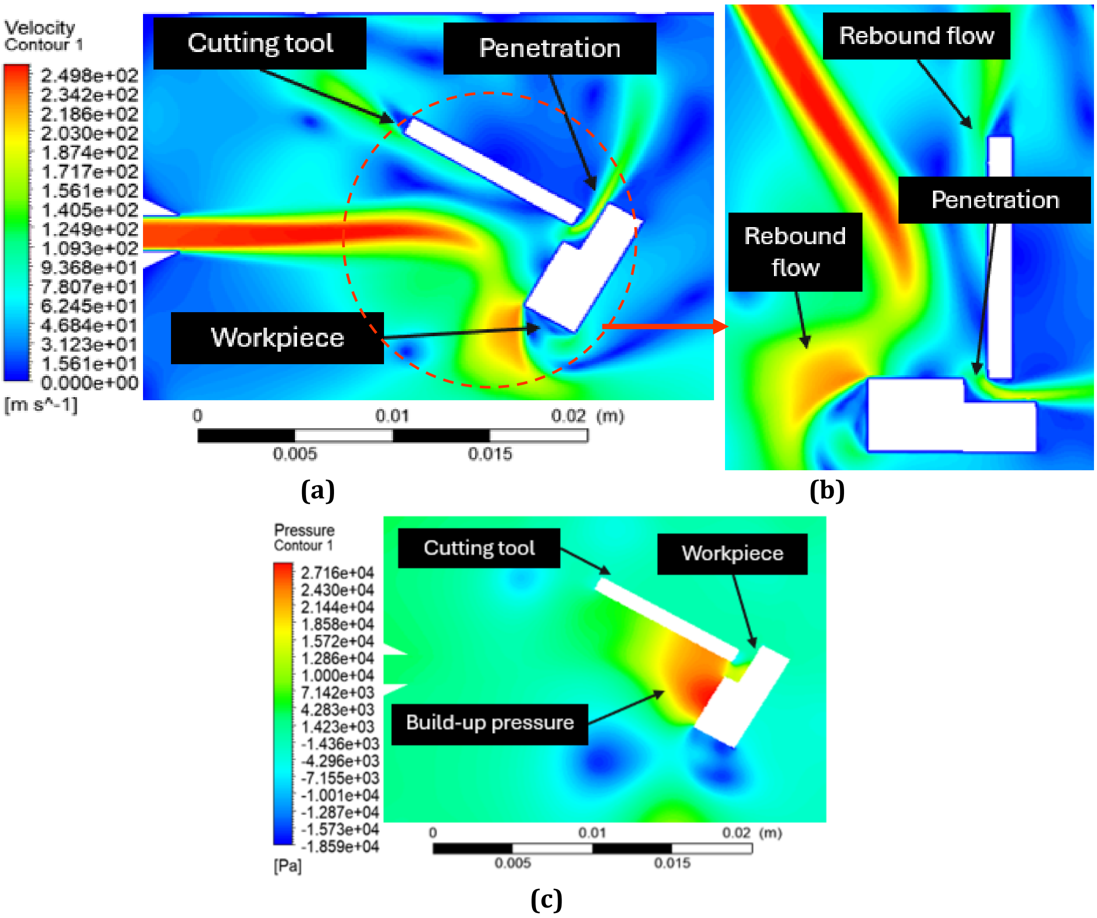

Fig. 6 *Simulation 2 with V: 115.52 m/s (Q:100 ml/hr, D: 2 mm, D: 20 mm); (a) Velocity contour; and (b) Pressure contour*

Figure 7a shows the CFD contour of the mist flow condition at a nozzle distance of 40 mm. Initially, the flow is in a steady phase before it turns to a dispersed phase as in mist form, where the mist becomes more turbulent as it travels toward the cutting area. This is believed to happen due to the flow losing its kinetic energy as it moves far from its energy source, which is from the centre line of the nozzle, as discussed by Rahim et al. [11]. At the turbulent regime of dispersed phase, the flow slowly loses its sharp pointed shape, and the dispersion of the flow becomes wider. This situation explains the reduction of flow velocity values, where it decreases as the flow travels along the distance. This condition also reduces the penetration of lubricant at the contact point as well as the cooling and lubricating effect by the MQL mist flow.

Referring to Figure 7b, the rebound effect happens around the cutting area but with lesser effect and concentration as compared to Figure 6b. Other than that, the concentration of the rebound can also be confirmed by the pressure contour in Figure 7c. The green-yellow contour pressure indicates a lower pressure value than in Figure 6c, meaning moderate turbulence occurs at the cutting zone.

When concerning actual cutting conditions, Zhu et al. [13] found that the increase in nozzle distance resulted in better machining performance. Through CFD analysis, they showed that it happens due to the reflow regime where the majority of the rebound droplets to rebound and re-adhesion to the contact surfaces. During machining, this condition will happen from the continuous flow of the MQL lubricant. Thus, it can be said that the rebound effect may have positive and negative effects depending on the proper combination of independent and dependent variables and cutting conditions.

From this analysis, it can be summarised that higher velocities are achieved with shorter nozzle distance, which is the most influential factor, followed by nozzle diameter and oil flow rates. A balance between the mist flow velocity and the rebound effect is important to ensure efficient mist flow penetration for better cooling and lubricating effect as well as chip removal. The lack of sufficient mist flow at the cutting zone may result in inefficient cooling and lubrication effects and the development of built-up edges (BUE) at the tool edge that will reduce machining performance [41].

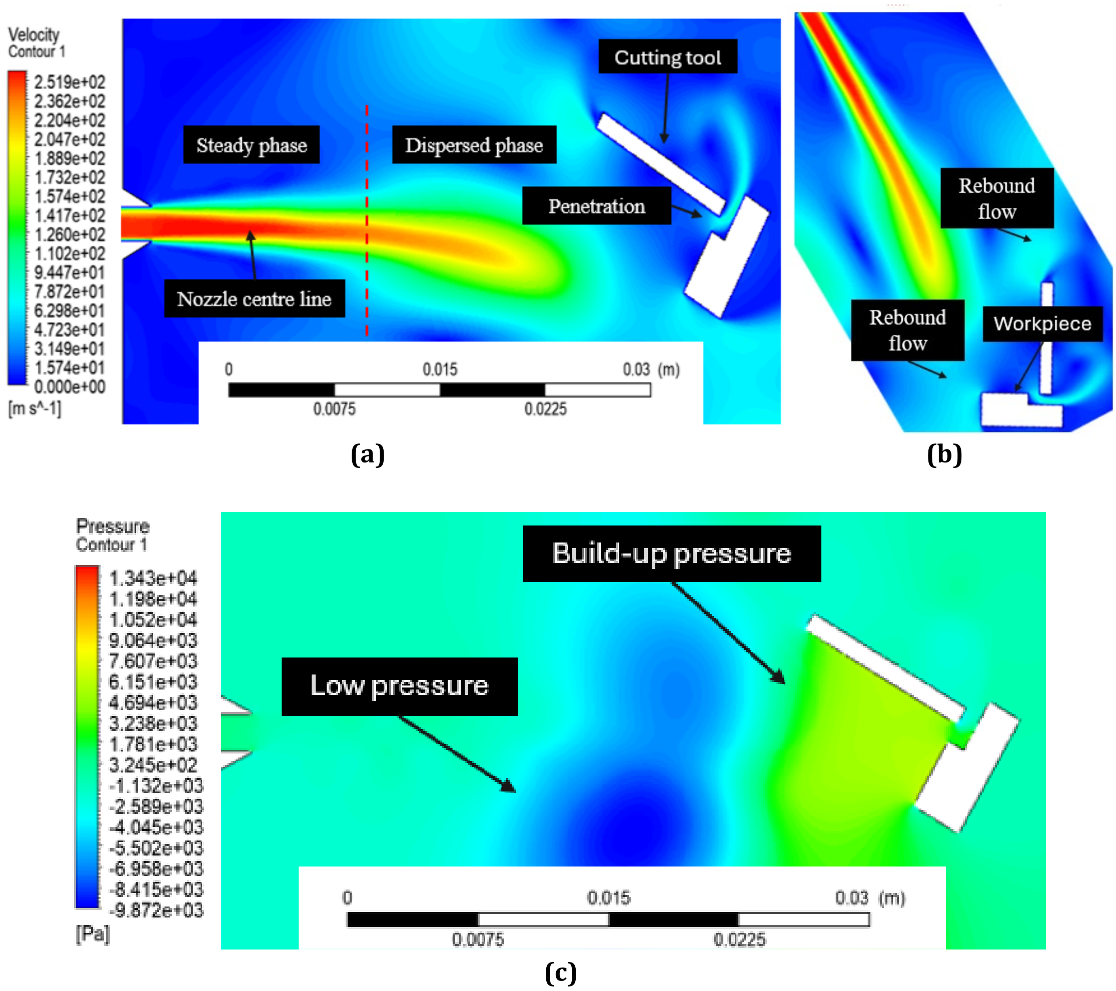

Fig. 7 *Simulation 13 (Q:150 ml/hr, D: 2 mm, D: 40 mm); (a) Velocity contour; and (b) Pressure contour*

Int. Journal of Integrated Engineering Vol. 16 No. 6 (2024) p. 294-309

3.5 Optimization and Validation of Optimum Parameters

The controlled factors of MQL mist flow are optimised to maximise the response, which is the MQL mist flow velocity. This is to ensure that the MQL mist efficiently penetrates the contact surfaces to provide sufficient lubrication, which is important to reduce friction and increase heat dissipation. At the same time, the high velocity of MQL mist flow is also required to help remove possible BUE formation onto the cutting edge during the cutting process.

The desirability approach is employed to optimise the response. Vera Candioti et al. [42] stated that the desirability functions as a principle for a model to indicate whether the model features are within or over the desirability limit. In this study, ANOVA suggested 100 solutions with different sets of optimum parameters and desirability values. Solution 11 with a desirability value of 1 for each controlled factor and response selected for this optimisation was chosen as shown in the ramp view in Figure 8. This optimum MQL parameter at Q: 100 ml/hr, D: 2 mm, and d: 20 mm suggests the optimum MQL mist flow velocity at 115.34 m/s. The desirability of 1 is a combination of all desirability from a single response and the factors are combined using a composite desirability function [43]. It also represents the ideal situation of this model, where an improvement beyond this point is impossible [20].

The confirmation test of single objective optimisation is conducted at the predicted optimal parameters to validate the predicted optimal output response through simulation. The analysis assesses the statistical significance of the difference between the simulated output response and the predicted output response of predicted optimal MQL parameters. The ANOVA outcomes indicated that the discrepancy between the predicted and optimal MQL parameters is not statistically significant, indicating that the single objective optimisation model is accurate with a difference percentage of 0.84%, which can be seen in Figure 9. The difference percentage is acceptable as the difference is less than 5% [44].

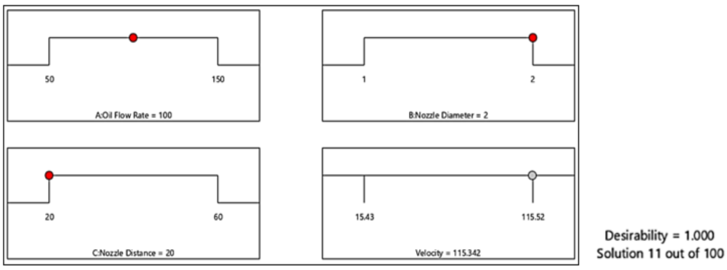

Fig. 8 *Ramp view of optimum MQL parameters*

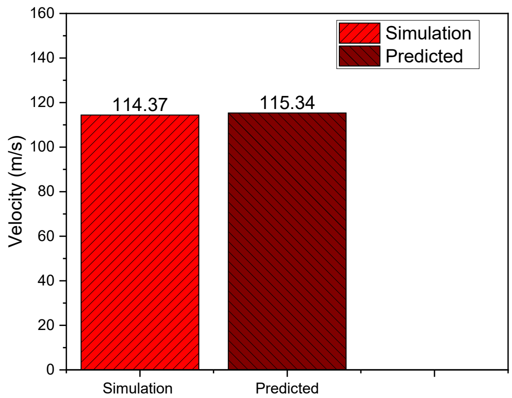

Fig. 9 *Comparison of velocity results between predicted and simulation*

4. Conclusion

This paper focuses on the sustainable method of MQL to optimise the mist flow velocity for efficient lubrication and penetration into the tool-workpiece interface by optimising the MQL parameters. The sustainability approach was enhanced using the Treated Recycled Cooking Oil (TRCO) biodegradable cutting fluid. The application of the MQL delivery system with the TRCO properties was performed through simulation work by CFD in Ansys Fluent. The ANOVA reported that the response of MQL mist flow velocity is significantly influenced by the nozzle distance, nozzle diameter, and interaction between them. It was found that the highest velocity mist flow is generated at a shorter nozzle distance with a larger nozzle diameter. In contrast, the lowest velocity is generated at a longer nozzle distance with a smaller nozzle diameter. A thorough analysis of the rebound and rebound conditions through CFD contour images showed that the highest velocity mist flow produced high rebound and rebound conditions, which contradicts the lowest velocity mist flow. This analysis helps to improve the MQL system to get better penetration through maximum velocity. In the optimisation, the optimum MQL parameters to maximise the MQL mist flow velocity are determined at Q: 100 ml/hr, D: 2mm, d: 20 mm by Box-Behnken RSM. The confirmation test was conducted with a difference percentage between the simulated and predicted outputs using the predicted optimal MQL parameters of 0.84%. In this study, the effective MQL nozzle distance was found to be between 20 mm and 40 mm, where any more or less than that will worsen the negative effect of rebound and hinder the ability of the mist flow to penetrate the cutting zone, causing insufficient cooling and lubrication.

Acknowledgement

We would like to express our gratitude to the Ministry of Higher Education (MOHE) Malaysia and Universiti Teknologi MARA, for providing research funds under the Fundamental Research Grant Scheme: Grant No. FRGS/1/2022/TK08/UITM/02/48 and 600- RMC/FRGS 5/3 (048/2022).

Conflict of Interest

Authors declare that there is no conflict of interests regarding the publication of the paper.

Author Contribution

The authors are responsible for the study conception, research design, data collection, data analysis, result interpretation and manuscript drafting.

References

[1] A. Shokrani, V. Dhokia, S. T. Newman, and R. Imani-Asrai (2012) An initial study of the effect of using liquid nitrogen coolant on the surface roughness of Inconel 718 nickel-based alloy in CNC milling, *Procedia CIRP*, *3*(1), 121–125, http://doi.org/10.1016/j.procir.2012.07.022

[2] O. Pereira, A. Celaya, G. Urbikaín, A. Rodríguez, A. Fernández-Valdivielso, and L. Noberto López de Lacalle (2020) CO2 cryogenic milling of Inconel 718: Cutting forces and tool wear, *Journal of Materials Research and Technology*, *9*(4), 8459–8468, 2020, http://doi.org/10.1016/j.jmrt.2020.05.118

[3] C. H. C. Haron, J. A. Ghani, M. F. Azhar, and N. H. A. Halim (2019) Wear mechanisms of coated tungsten carbide when machining Inconel 718 under cryogenic and dry conditions, *Jurnal Tribology*, *22*, 108–116,

[4] P. Shah, P. Bhat, and N. Khanna (2021) Life cycle assessment of drilling Inconel 718 using cryogenic cutting fluids while considering sustainability parameters, *Sustainable Energy Technologies and Assessments*, *43*, 1–16, http://doi.org/10.1016/j.seta.2020.100950

[5] P. B. Zaman and N. R. Dhar (2019) Design and evaluation of an embedded double jet nozzle for MQL delivery intending machinability improvement in turning operation, *Journal of Manufacturing Processes*, *44*, 179–196, http://doi.org/0.1016/j.jmapro.2019.05.047

[6] M. G. Faga, P. C. Priarone, M. Robiglio, L. Settineri, and V. Tebaldo (2017) Technological and sustainability implications of dry, near-dry, and wet turning of Ti-6Al-4V alloy, *International Journal of Precision Engineering and Manufacturing - Green Technology*, *4*(2), 129–139, 2017, http://doi.org/10.1007/s40684-017-0016-z

[7] Z. Said, M. Gupta, H. Hegab, N. Arora, A. M. Khan, M. Jamil, and E. Bellos (2019) A comprehensive review on minimum quantity lubrication (MQL) in machining processes using nano-cutting fluids, *International Journal of Advanced Manufacturing Technology*, *105*(5-6), 2057–2086, http://doi.org/10.1007/s00170-019-04382-x

[8] A. S. Awale, M. Vashista, and M. Z. Khan Yusufzai (2020) Multi-objective optimization of MQL mist parameters for eco-friendly grinding, *Journal of Manufacturing Processes*, *56*, 75–86, http://doi.org/10.1016/j.jmapro.2020.04.069

[9] N. H. Abdul Halim, C. H. Che Haron, and J. Abdul Ghani (2020) Sustainable machining of hardened Inconel 718: a comparative study, *International Journal of Precision Engineering and Manufacturing*, *21*(7), 1375–1387, http://doi.org/10.1007/s12541-020-00332-w

[10] K. L. J. Kiat, N. I. K. Ismail, N. Rosli, and E. A. Alias (2021) Study of nozzle distance and oil flow rate effects on the droplets size of minimum quantity lubrication," *IOP Conference Series: Materials Science and Engineering*, *1062*(1), 1-12, http://doi.org/10.1088/1757-899X/1062/1/012006

[11] E. A. Rahim, H. Dorairaju, N. Asmuin, and M. H. A. R. Mantari (2015) Determination of mist flow characteristic for mql technique using particle image velocimetry (PIV) and computer fluid dynamics (CFD), *Applied Mechanics Materials*, 773–774, 403–407, http://doi.org/10.4028/www.scientific.net/amm.773-774.403

[12] E. A. Rahim and H. Dorairaju (2018) Evaluation of mist flow characteristic and performance in Minimum Quantity Lubrication (MQL) machining, *Measurement: Journal of the International Measurement Confederation*, *123*, 213–225, http://doi.org/10.1016/j.measurement.2018.03.015
[13] G. Zhu, S. Yuan, and B. Chen (2019) Numerical and experimental optimizations of nozzle distance in minimum quantity lubrication (MQL) milling process, *International Journal of Advanced Manufacturing Technology*, *101*(1–4), 565–578, http://doi.org/10.1007/s00170-018-2928-3
[14] Z. Zan, K. Guo, J. Sun, X. Wei, Y. Tan, and B. Yang (2021) Investigation of MQL parameters in milling of titanium alloy, *International Journal of Advanced Manufacturing Technology*, *116*(1–2), 375–388, http://doi.org/10.1007/s00170-021-07441-4
[15] T. Tawakoli, M. J. Hadad, and M. H. Sadeghi (2010) Influence of oil mist parameters on minimum quantity lubrication - MQL grinding process, *International Journal of Machine Tools and Manufacture*, *50*(6), 521–531, http://doi.org/10.1016/j.ijmachtools.2010.03.005
[16] W. El-Bouri, I. Deiab, K. Khanafer, and E. Wahba (2019) Numerical and experimental analysis of turbulent flow and heat transfer of minimum quantity lubrication in a turning process using discrete phase model, *International Communications in Heat and Mass Transfer*, *104*, 23–32, http://doi.org/10.1016/j.icheatmasstransfer.2019.02.012
[17] Z. Q. Liu, X. J. Cai, M. Chen, and Q. L. An (2011) Investigation of cutting force and temperature of end-milling Ti-6Al-4V with different minimum quantity lubrication (MQL) parameters, in *Proceedings of the Institution of Mechanical Engineers, Part B: Journal of Engineering Manufacture*, *225*(8), 1273–1279, http://doi.org/10.1177/2041297510393793
[18] C. D. Wang, M. Chen, Q. L. An, M. Wang, and Y. H. Zhu (2014) Tool wear performance in face milling Inconel 182 using minimum quantity lubrication with different nozzle positions, *International Journal of Precision Engineering and Manufacturing*, *15*(3), 557–565, http://doi.org/10.1007/s12541-014-0371-4
[19] O. Pereira, A. Rodríguez, J. Barreiro, A. I. Fernández-Abia, and L. N. L. de Lacalle (2017) Nozzle design for combined use of MQL and cryogenic gas in machining, *International Journal of Precision Engineering and Manufacturing - Green Technology*, *4*(1), 87–95, http://doi.org/10.1007/s40684-017-0012-3
[20] P. B. Zaman and N. R. Dhar (2020) Multi-objective Optimization of Double-Jet MQL System Parameters Meant for Enhancing the Turning Performance of Ti–6Al–4V Alloy, *Arabian Journal for Science and Engineering*, *45*(11), 9505–9526, http://doi.org/10.1007/s13369-020-04806-x
[21] K. Khanafer, I. Deiab, and W. El-Bouri (2020) Numerical analysis of flow and heat transfer of minimum quantity lubrication in a turning process using Inconel alloy, *International Journal of Advanced Manufacturing and Technology*, *108*, 475–483, 2020
[22] Y. You, S. Wang, W. Lv, Y. Chen, and U. Gross (2021) A CFD model of frost formation based on dynamic meshes technique via secondary development of ANSYS fluent, *International Journal of Heat and Fluid Flow*, *89*, 1–8, http://doi.org/10.1016/j.ijheatfluidflow.2021.108807
[23] M. S. Najiha, M. M. Rahman, M. Kamal, A. R. Yusoff, and K. Kadirgama (2012) Minimum quantity lubricant flow analysis in end milling process: A computational fluid dynamics approach, *Journal of Mechanical Engineering and Sciences*, *3*, 340–345.
[24] M. S. Najiha, M. M. Rahman, A. R. Yusoff, and K. Kadirgama (2012) Investigation of flow behavior in minimum quantity, *International Journal of Automotomotive and Mechanical*, *6*, 768–776.
[25] S. Subramani, S. Nantha Muthu, and N. L. Gajbhiye (2022) A numerical study on the influence of minimum quantity lubrication parameters on spray characteristics of rapeseed oil as cutting fluid, *Industrial Lubrication and Tribology*, *74*(2), 197–204, http://doi.org/10.1108/ILT-08-2021-0305
[26] Z. Zulkifli, N. H. A. Halim, Z. H. Solihin, J. Saedon, A. A. Ahmad, A. H. Abdullah, N. A. Raof, and M. A. Hadi (2023) The analysis of grid independence study in continuous disperse of MQL delivery system, *Journal of Mechanical Engineering and Sciences*, *17*(3), 9586–9596,
[27] S. M. Mousavi, A. Jafari, S. Chegini, and I. Turunen (2009), CFD simulation of mass transfer and flow behaviour around a single particle in bioleaching process, *Process Biochemistry*, *44*(7), 696–703, http://doi.org/ 10.1016/j.procbio.2009.02.016
[28] A. A. Ahmad, J. A. Ghani, and C. H. Che Haron (2022) Effect of cutting parameters on tool life during end milling of AISI 4340 under MQL condition, *Industrial Lubrication and Tribology*, *74*(4), 392–401, http://doi.org/10.1108/ILT-08-2021-0295
[29] Y. Xu, J. Yuan, J. U. Repke, and G. Wozny (2012) CFD study on liquid flow behavior on inclined flat plate focusing on effect of flow rate, *Engineering Applications of Computational Fluid Mechanics*, *6*(2), 186–194, http://doi.org/10.1080/19942060.2012.11015413
[30] A. S. Putri, R. Amalia, T. H. Ariwibowo, and F. H. Sholihah (2021) Thermal characteristics of tube economizer with serrated fin, *Internationa Electronics Symposium 2021: Wireless Technology and Intelligent System Better Human Lives, IES 2021 - Proceedings*, 399–404, http://doi.org/10.1109/IES53407.2021.9593988

[31] J. D. Kechagias, K. E. Aslani, N. A. Fountas, N. M. Vaxevanidis, and D. E. Manolakos (2020) A comparative investigation of Taguchi and full factorial design for machinability prediction in turning of a titanium alloy, *Measurement: Journal of the International Measurement Confederation*, *151*, 1-20, http://doi.org/10.1016/j.measurement.2019.107213
[32] A. Le Van and T. T. Nguyen (2022) Investigation and optimization of mql system parameters in the roller-burnishing process of hardened steel," *Journal of Mechanical Engineering*, *68*(3), 155–165, http://doi.org/10.5545/sv-jme.2021.7473
[33] X. Wang, C. Li, Y. Zhang, W. Ding, M. Yang, T. Gao, H. Cao, X. Xu, D. Wang, Z. Said, S. Debnath, M. Jamil, and H. M. Ali (2020) Vegetable oil-based nanofluid minimum quantity lubrication turning: Academic review and perspectives, *Journal of Manufacturing Processes*, *59*, 76–97, http://doi.org/10.1016/j.jmapro.2020.09.044
[34] V. Shaikh, N. Boubekri, and T. W. Scharf (2014) Analyzing the effectiveness of microlubrication using a vegetable oil-based metal working fluid during end milling aisi 1018 steel, *International Journal of Manufacturing Engineering*, 2014, 1–13, http://doi.org/10.1155/2014/261349
[35] R. Hills and T. Trucano (2005) Statistical validation of engineering and scientific models: Background, *Sandia National Laboratories, SAND99*, 1-18
[36] M. Chen, L. Jiang, B. Shi, Z. Liu, and Q. An (2012) CFD analysis on the flow field of minimum quantity lubrication during external thread turning, in *Materials Science Forum*, *723*, 113–118, http://doi.org/10.4028/www.scientific.net/MSF.723.113
[37] Warjito, Budiarso, I. A. Pramono, M. L. Samosir, and D. Adanta (2019) The effect of nozzle diameter on the flow characteristics of air entrainment phenomenon in vertical plunging jets, *AIP Conference Proceedings,* 2062, 1-9, http://doi.org/10.1063/1.5086573
[38] W. Seehanam, K. Pianthong, W. Sittiwong, and B. Milton (2014) Injection pressure and velocity of impact-driven liquid jets, *Engineering Computations (Swansea, Wales)*, *31*(7), 1130–1150, http://doi.org/10.1108/EC-09-2012-0218
[39] W.-Y. Yang, J.-C. Yang, and I.-H. Sung (2011) A study of the effects of pressure velocity and fluid viscosity in abrasive machining process, *Journal of the Korean Society of Tribologist Lubrication Engineers*, *27*(1), 7–12, http://doi.org/10.9725/kstle.2011.27.1.007
[40] W. T. Urmi, M. M. Rahman, W. Safiei, K. Kadirgama, and M. A. Maleque (2022) Effects of minimum quantity lubrication technique in different machining processes -A comprehensive review, *Journal of Advanced Research in Fluid Mechanics and Thermal Sciences*, *90*(2), 135–159, http://doi.org/10.37934/arfmts.90.2.135159
[41] Y. Kamata, T. Obikawa, and J. Shinozuka (2004) Analysis of mist flow in mql cutting, *Key Engineering Materiasl*, *258*, 339–344, http://doi.org/10.4028/www.scientific.net/KEM.257-258.339
[42] L. Vera Candioti, M. M. De Zan, M. S. Cámara, and H. C. Goicoechea (2014) Experimental design and multiple response optimization. Using the desirability function in analytical methods development, *Talanta*, *124*, 123–138, http://doi.org/10.1016/j.talanta.2014.01.034
[43] B. Davoodi and B. Eskandari (2015) Tool wear mechanisms and multi-response optimization of tool life and volume of material removed in turning of N-155 iron-nickel-base superalloy using RSM, *Measurement: Journal of the International Measurement Confederation*, *68,* 286–294, http://doi.org/10.1016/j.measurement.2015.03.006
[44] A. Thakur, V. Guleria, and R. Lal (2022) Multi-response optimization in turning of EN-24 steel under MQL, *Engineering Research Express*, *4*(2), http://doi.org/10.1088/2631-8695/ac7a0c